Electronic Structure of the Superconducting Rare-Earth-Metal Nickel Boron Carbide Compounds

Jean-François Halet

Laboratoire de Chimie du Solide et Inorganique Moléculaire, URA CNRS 1495, Université de Rennes I, 35042 Rennes, France

Received April 8, 1994®

An analysis of the electronic structure and bonding in the superconducting $LnNi_2B_2C$ and nonsuperconducting LnNiBC phases is made, using extended Hückel tight-binding calculations. The results show that these compounds are highly covalent and can be considered as intermetallic materials. Oxidation formalisms of $(Ln^{2+})(Ni^0)_2(B_2C)^{2-}$ for $LnNi_2B_2C$ and $(Ln^{3+})(Ni^0)(BC)^{3-}$ for LnNiBC constitute good starting points to describe their electronic structure. The Fermi level cuts a narrow and sharp peak in the DOS for $LuNi_2B_2C$, mainly composed of σ-type Ni—B bonding states. This allows us to conclude that electrons transferred from the $(B_2C)^{2-}$ entities into σ-type metal–non-metal bonding states are responsible for the superconducting properties encountered for certain $LnNi_2B_2C$ compounds. Flat bands are calculated in the planes perpendicular to the stacking c axis. These materials should be 2-D-like superconductors. The absence of superconductivity for LuNiBC seems to be associated with the rather weak DOS at the Fermi level, compared to that of $LuNi_2B_2C$.

Relatively high-transition temperatures (T_c's) up to 23 K have been reported for some rare-earth-metal transition-metal boron carbide compounds.[1-4] Although their T_c values are far below those measured for the copper oxide superconductors,[5] these new quaternary intermetallic materials could constitute milestones in terms of the discovery of a new family of high-T_c superconductors. We report here the band electronic structure of the well-characterized $LnNi_2B_2C$ compounds,[6] some of which exhibit superconductivity above 15 K,[4] using tight-binding calculations.[7]

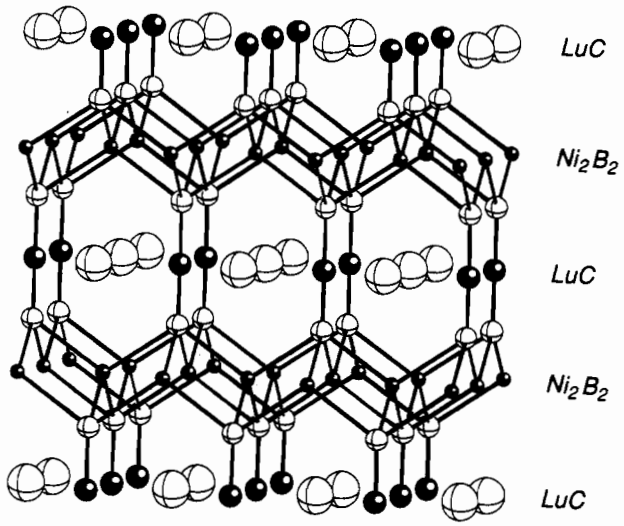

Figure 1. Crystal structure of $LuNi_2B_2C$.

A comparison is made with the structure of the nonsuperconducting related phase LuNiBC.[8]

The crystal structure of $LnNi_2B_2C$ (Ln = Y, La, Ce, Sm, Tb, Dy, Ho, Er, Tm, Lu) can be regarded as a "stuffed" variant of the tetragonal body-centered $ThCr_2Si_2$-type structure (see Figure 1), composed of inverse PbO-type Ni_2B_2 slabs alternating with NaCl-type LnC sheets.[6] Strong covalent interactions betwen the Ni_2B_2 and LnC layers lead to the formation of tightly bound linear B–C–B units, which confer a 3-D character upon the material. An alternative way to look at the structure of $LnNi_2B_2C$ is to consider a set of isolated B_2C units trapped in holes formed by the $LnNi_2$ metallic matrix. The B–C separations (1.47 Å in $LuNi_2B_2C$) suggest a double-bond character between B and C. Triatomic entities of main-group elements burried in a metallic matrix are not unprecedented in solid state chemistry,[9] particularly in ternary rare-earth-metal boron carbide compounds[10,11] such as Sc_2BC_2[12] or $La_5B_2C_6$,[13] which contain linear C–B–C units with comparable B–C bond distances. Some of them, like $La_5B_2C_6$, are even superconducting up to 6.9 K.[13,14]

® Abstract published in *Advance ACS Abstracts,* August 1, 1994.

(1) Mazumdar, C.; Nagarajan, R.; Godart, C.; Gupta, L. C.; Latroche, M.; Dhar, S. K.; Levy-Clément, C.; Padalia, B. D.; Vijayaraghavan, R. *Solid State Commun.* **1993**, *87*, 413.
(2) Nagarajan, R.; Mazumdar, C.; Hossain, Z.; Dhar, S. K.; Gopalakrishnan, K. V.; Gupta, L. C.; Godart, C.; Padalia, B. D.; Vijayaraghavan, R. *Phys. Rev. Lett.* **1994**, *72*, 274.
(3) Cava, R. J.; Takagi, H.; Batlogg, B.; Zandbergen, H. W.; Krajewski, J. J.; Peck, W. F.; van Dover, R. B.; Felder, R. J.; Siegrist, T.; Mizuhashi, K.; Lee, J. O.; Elsaki, H.; Carter, S. A.; Uchida, S. *Nature* **1994**, *367*, 146.
(4) Cava, R. J.; Takagi, H.; Zandbergen, H. W.; Krajewski, J. J.; Peck, W. F., Jr.; Siegrist, T.; Batlogg, B.; van Dover, R. B.; Felder, R. J.; Mizuhashi, K.; Lee, J. O.; Elsaki, H.; Uchida, S. *Nature* **1994**, *367*, 252.
(5) See for example Laguës, M.; Xie, X. M.; Tebbji, H.; Xu, X. Z.; Mairet, V.; Hatterer, C.; Beurau, C. F.; Deville-Cavellin, C. *Science (Washington, D.C.)* **1993**, *262*, 1850.
(6) Siegrist, T.; Zandbergen, H. W.; Cava, R. J.; Krajewski, J. J.; Peck, W. F., Jr. *Nature* **1994**, *367*, 254. See also: Hong, N. M.; Michor, H.; Vybornov, M.; Holubr, T.; Hundegger, P.; Perthold, W.; Hilscher, G.; Rogl, P. *Physica C*, in press (for YNi_2B_2C).
(7) Molecular and tight-binding calculations were carried out within the extended Hückel formalism: (a) Hoffmann, R. *J. Chem. Phys.* **1963**, *39*, 1397. (b) Whangbo, M.-H.; Hoffmann, R. *J. Am. Chem. Soc.* **1978**, *100*, 6093. Different sets of parameters for the rare-earth-metal atoms were used. They basically led to the same qualitative conclusions. We chose to present here the results obtained with the parameters of lutetium. The role of the rather contracted f orbitals has been neglected, and thus they were not included in the calculations. The exponent (ζ) and the valence shell ionization potential (H_{ii} in eV) were respectively as follows: 1.3, −15.2 for B 2s; 1.3, −8.5 for B 2p; 1.625, −21.4 for C 2s; 1.625, −11.4 for C 2p; 2.1, −9.17 for Ni 4s; 2.1, −6.27 for Ni 4p; 1.39, −8.6 for Lu 6s; 1.39, −5.0 for Lu 6p. H_{ii} values for Ni 3d and Lu 5d were set equal to −13.49 and −8.4 eV, respectively. A linear combination of two Slater-type orbitals of exponents $\zeta_1 = 5.75$, $\zeta_2 = 2.0$ and $\zeta_1 = 4.33$, $\zeta_2 = 1.4$ with weigthing coefficients $c_1 = 0.5683$, $c_2 = 0.6292$ and $c_1 = 0.5827$, $c_2 = 0.6772$ was used to represent the 3d and 5d atomic orbitals of Ni and Lu, respectively. The crystal structures of $LuNi_2B_2C$ and LuNiBC were used for the calculations. Sets of 40K points chosen in the corresponding irreducible Brillouin zone were utilized for the calculations of the density of states, overlap populations, and atomic net charges.
(8) (a) Mattheiss, L. F. *Phys. Rev. B*, in press. (b) Pickett, W. E.; Singh, D. J. *Phys. Rev. Lett.* **1994**, *72*, 3702.
(9) See for example: Womelsdorf, H.; Meyer, H.-J. *Z. Anorg. Allg. Chem.* **1994**, *620*, 262 and references therein.
(10) Wiitkar, F.; Halet, J.-F.; Saillard, J.-Y.; Bauer, J.; Rogl, P. *J. Am. Chem. Soc.* **1994**, *116*, 251.
(11) Zouchoune, B.; Halet, J.-F.; Saillard, J.-Y.; Bauer, J. To be submitted for publication.
(12) Halet, J.-F.; Saillard, J.-Y.; Bauer, J. *J. Less-Common Met.* **1990**, *158*, 239.
(13) Bauer, J.; Bars, O. *J. Less-Common Met.* **1983**, *95*, 267.
(14) Bauer, J.; Politis, C. *J. Less-Common Met.* **1982**, *88*, L1.

0020-1669/94/1333-4173$04.50/0

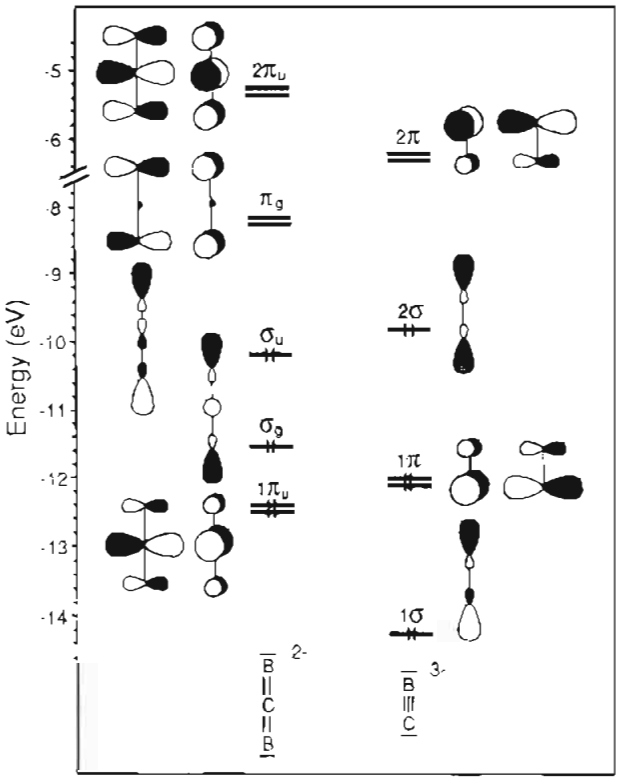

Figure 2. EH MO diagram for the isolated $(B_2C)^{2-}$ and $(BC)^{3-}$ entities.

The Electronic Structure of $LuNi_2B_2C$

The assignment of formal oxidation states of the elements constituting a given compound is a useful starting point to tackle its electronic structure. A comparison of the electronegativity of the different elements present in the $LuNi_2B_2C$ phase leads us to propose a formal charge distribution $(Lu^{3+})(Ni^0)(B_2C)^{3-}$.

The atomic orbitals (AOs) of the boron and carbon atoms constituting an isolated B_2C entity combine to give the molecular orbital diagram shown on the left-hand side of Figure 2. Mixing of the 2s and one 2p AOs leads to six σ-type molecular orbitals (MOs): two B–C strongly bonding, two nonbonding, and, very high in energy, two strongly antibonding. Only the nonbonding combinations σ_g and σ_u are shown in Figure 2. The other 2p AOs form pairs of degenerate B–C bonding ($1\pi_u$), nonbonding (π_g), and antibonding ($2\pi_u$) π-type MOs. The large gap computed between the nonbonding π_g and antibonding $2\pi_u$ MOs (3.09 eV) would lead us to assign a count of 16 electrons for the isolated B_2C unit, i.e. a formal charge of 6–. This would render the $(B_2C)^{6-}$ entity isoelectronic with CO_2, or $(BC_2)^{5-}$ in Sc_2BC_2[12] and $La_5B_2C_6$,[13] or $(C_3)^{4-}$ in Sc_3C_4,[15] with formal B–C double bonds and atoms following the octet rule. However, such an important anionic charge for B_2C seems inadequate for at least two reasons. First, the nonbonding π_g MOs are fairly high in energy to be occupied. Second, such a charge renders the atoms positioned at the end of the linear triatomic entity strongly negatively charged compared to that of the central one. Indeed, keeping the same atomic separations, extended Hückel calculations show that the "asymmetrical" C–B–B distribution, i.e. with one B atom at the center of the molecule, is largely preferred by ca. 4.5 eV with a HOMO–LUMO gap of 5.71 eV for the charge of 6–. However,

Table 1. Characteristics Computed for the $LuNi_2B_2C$ and LuNiBC Compounds

	$LuNi_2B_2C$		LuNiBC
	Fermi Levels (eV)		
	–9.616		–10.085
	Overlap Populations		
Ni–Ni	0.138		0.132
Ni–B	0.304		0.291
B–C	1.023		0.977
Lu–B	0.072		0.053
Lu–C	0.157		0.241
Lu–C[a]			0.394
	Atomic Net Charges		
Lu	+1.48		+1.24
Ni	–0.50		–0.28
B	+0.35		+0.50
C	–1.18		–1.46
(B_2C)[b]	–0.48		
(BC)[c]			–0.94
	FMO Occupations		
(B_2C) $1\pi_u$	3.30	(BC) 1σ	1.35
(B_2C) σ_g	1.04	(BC) 1π	3.07
(B_2C) σ_u	1.14	(BC) 2σ	1.16
(B_2C) π_g	0.90	(BC) 2π	0.50
(B_2C) $2\pi_u$	0.36		

[a] Separation between Lu–C sheets. [b] In $LuNi_2B_2C$. [c] In LuNiBC.

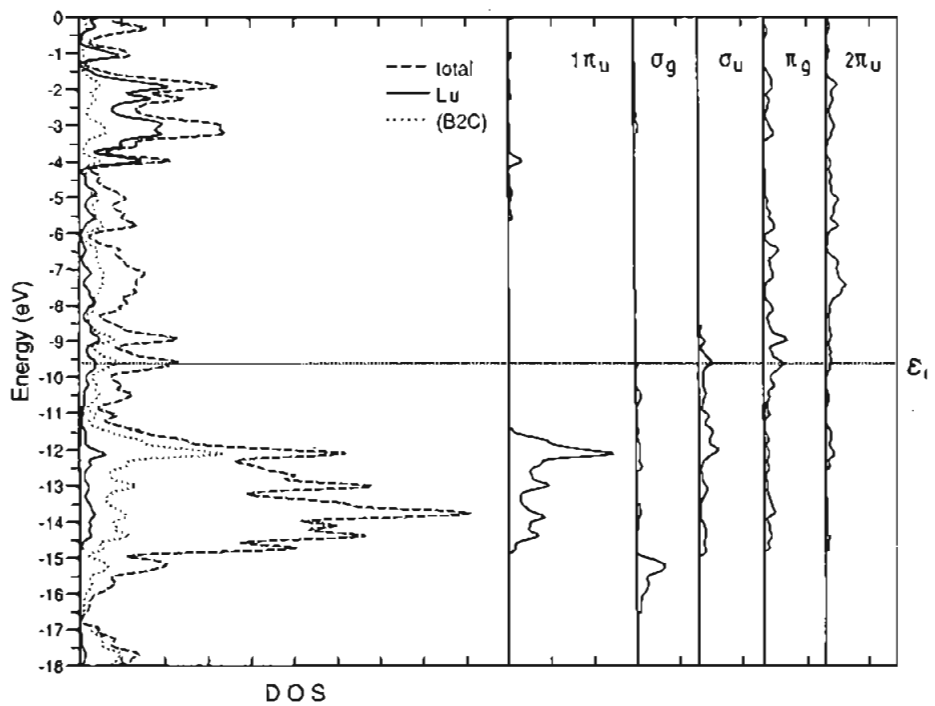

Figure 3. Left: Densities of states: total (dashed line); Lu (solid line); B_2C (dotted line). Right: B_2C FMO contributions for $LuNi_2B_2C$.

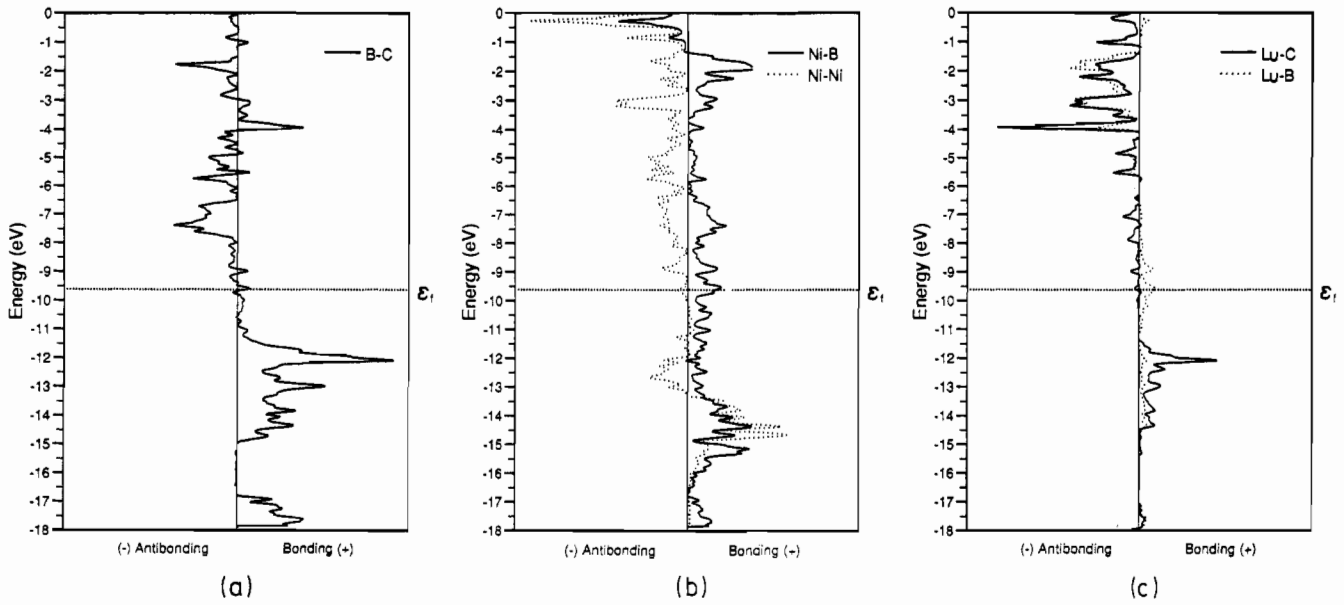

Figure 4. COOP curves for (a) B–C, (b) Ni–B (solid line) and Ni–Ni (dotted line), and (c) Lu–C (solid line) and Lu–B (dotted line) contacts in $LuNi_2B_2C$.

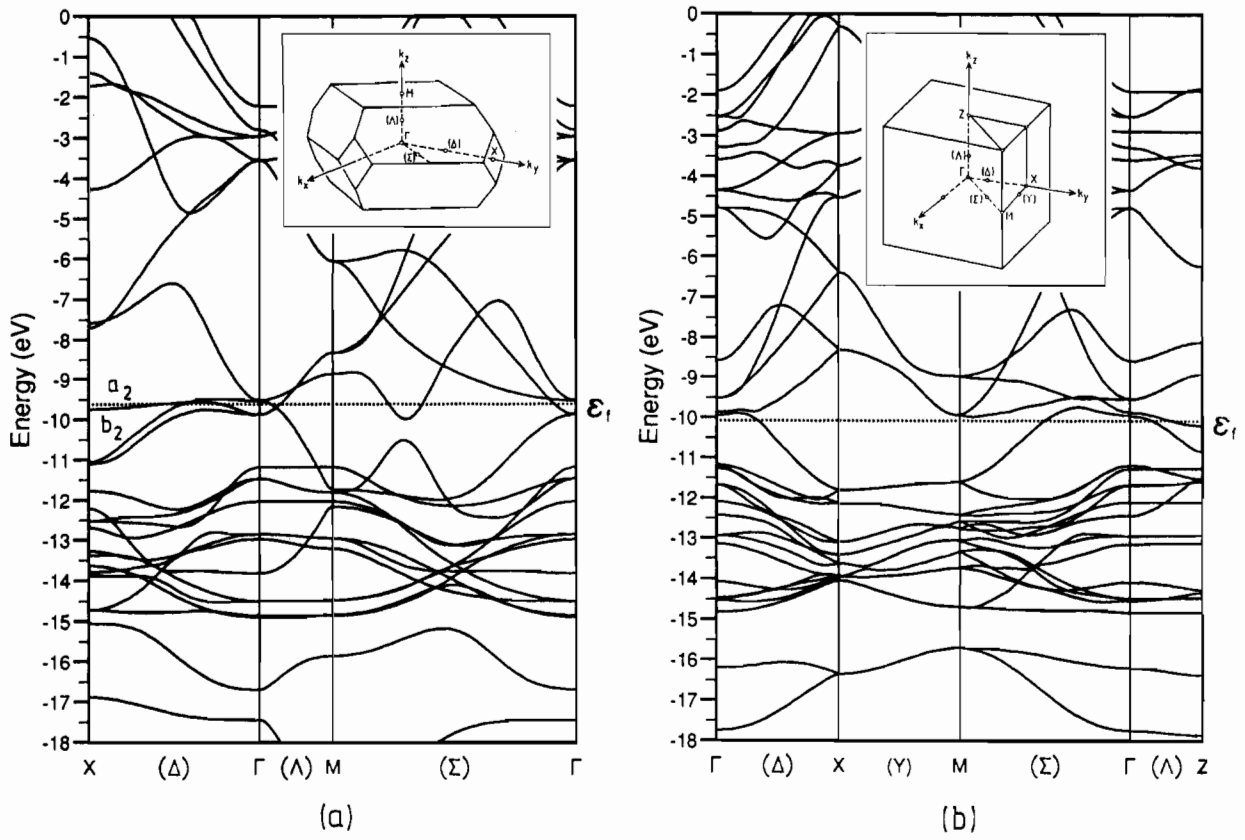

Figure 5. Band structures of (a) $LuNi_2B_2C$ and (b) LuNiBC.

such a distribution would induce some disorder or a lowering of symmetry in the solid state, with Ni_2B_2 and Ni_2C_2 layers alternating with LuB sheets. This has not been observed by Siegrist *et al.*, who propose without any ambiguity that the less electronegative atoms, namely boron, occupy the end sites rather than the center site in the B_2C units of $LuNi_2B_2C$.[6] On the other hand, for a charge of 2– per entity, i.e. with the nonbonding π_g MOs depopulated, the symmetrical B–C–B arrangement becomes slightly preferred. Such a charge would lead to six-electron terminal B atoms, often encountered in molecular and solid state boron chemistry. Note that a rather important HOMO–LUMO gap persists (1.88 eV) and that the double-bond character is retained for the charge of 2– per B_2C. Therefore, on the basis of the MO diagram of B_2C, the charge distribution $(Lu^{2+})(Ni^0)(B_2C)^{2-}$ constitutes a good oxidation state formalism to start with.

Covalent interactions between the metal atoms Lu^{2+} and Ni^0 and the $(B_2C)^{2-}$ entities must reduce somewhat the anionic charge of the last. The density of states (DOS) for $LuNi_2B_2C$ is shown in Figure 3. The DOS separates broadly into three parts. A decomposition of the contribution to the DOS of the different elements indicates that the lowest part, centered at –13 eV, derives mainly from the nickel atoms and to a less extent from the B_2C entities. The highest part of the DOS, centered around –3 eV, is composed mainly of lanthanide atoms. The top of the former

(15) Meyer, H.-J.; Hoffmann, R. *Z. Anorg. Allg. Chem.* **1992**, *607*, 57.

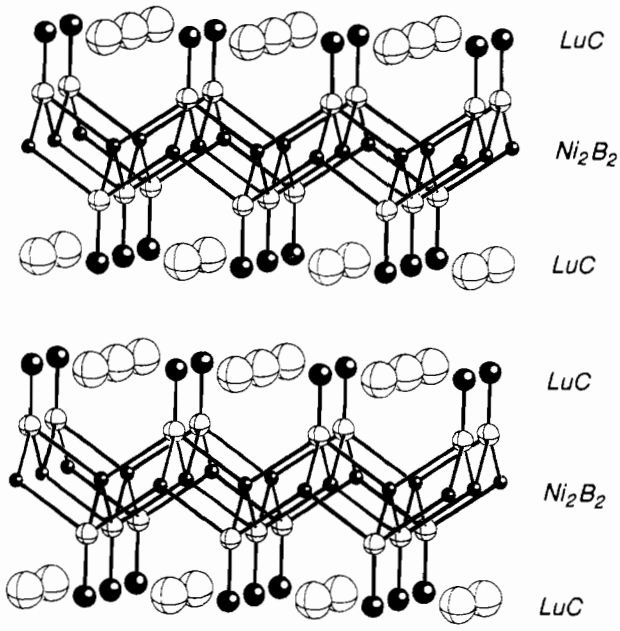

Figure 6. Crystal structure of LuNiBC.

and the bottom of the latter are highly dispersed and overlap considerably, leading to the formation of small peaks of DOS intercalated between these two wide bands. A participation of the B_2C entities is observed throughout the energy range.

The Fermi level ($\mathcal{E}_F$) sits at the very top of the Ni d band in a particularly narrow and sharp peak. The analysis of this peak reveals a participation of all the components (Lu, Ni, B_2C) of $LuNi_2B_2C$. According to the projected DOS of the B_2C molecular frontier orbitals (FMO) shown in Figure 3, the B_2C contribution arises essentially from the nonbonding π_g and σ_u FMOs exclusively and mainly localized on the B atoms, respectively (see Table 1 for the B_2C FMO occupation after interaction with the metallic framework). The small but nonnegligible participation of the B–C antibonding $2\pi_u$ states is responsible for the weak participation of C in this peak of DOS. This weak C contribution at the Fermi level has also been noticed by Mattheiss, who studied the electronic structure of $LuNi_2B_2C$ in the local-density approximation using the linear augmented-plane wave method.[8a] It is noteworthy that the same phenomenon, i.e. participation of nonbonding and/or antibonding FMOs of the non-metal units accompanied by a metallic contribution at the Fermi level, occurs also in Sc_2BC_2[12] and in the superconducting $La_5B_2C_6$ compound.[11] It is also observed in the layered rare-earth-metal carbide halides, containing C_2 entities, some of which are superconducting.[16]

The computed atomic net charges reported in Table 1 reflect some electron transfer from the anionic B_2C units toward the Ni and Lu atoms. These strong covalent interactions between the different elements in the material manifest themselves also through the different atomic overlap populations, which are highly positive (see Table 1). Their corresponding crystal orbital overlap population (COOP)[17] curves, given in Figure 4, indicate that some of them are not maximized. For instance, Ni–B and Lu–B COOP curves are still bonding above the Fermi level. The addition of extra electrons would enhance these contacts. The rather important depopulation of the B–C nonbonding σ_u and σ_g FMOs of the B_2C units after interaction hardly affects the strength of the B–C double bonds. The actual B–C overlap population computed for the solid is 1.023, not too different from that calculated for the isolated $(B_2C)^{2-}$ entity, which is 1.283. This is confirmed by the B–C COOP curve represented in Figure 4a, which shows that nearly all the B–C bonding states are occupied after interaction.

As shown from the band structure given in Figure 5, the narrow peak of DOS cut by $\mathcal{E}_F$ comes primarily from flat and nearly half-filled bands of symmetries a_2 and b_2 under C_{2v} symmetry, running along the line Δ ($\Gamma \rightarrow X$), which corresponds to the [110] direction in the crystal. A closer look at these a_2 and b_2 bands indicates that both are σ-type nickel–B_2C bonding overall with a participation of B_2C through the nonbonding π_g and σ_u FMOs in the former and the latter, respectively. A small π-type Lu–C antibonding contribution is noted in the b_2 band. Sketches of these bands at the high-symmetry point Γ are given by **1** and **2** (they are essentially the same at X). $\mathcal{E}_F$ crosses more dispersive bands along the line Λ ($\Gamma \rightarrow M$) corresponding to the stacking c axis in the crystal. Some of them possess some B_2C $2\pi_u$ contribution.

The Electronic Structure of LuNiBC

The addition of a supplementary Lu–C layer to the structure of $LuNi_2B_2C$ leads to the nonsuperconducting compound LuNiBC,[6] which contains isolated non-metal BC units and is

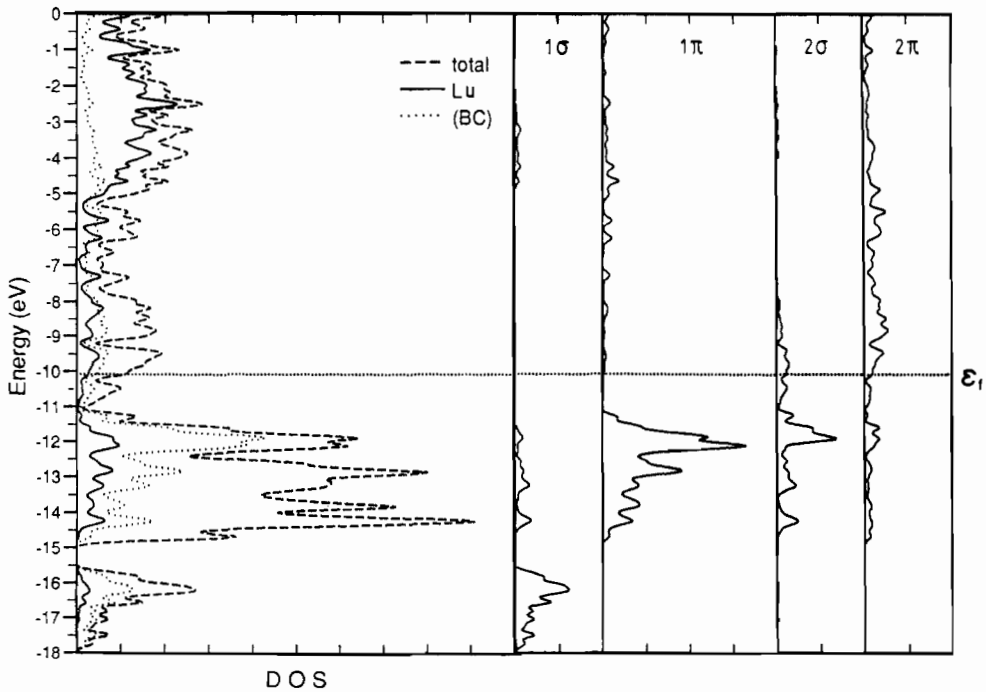

Figure 7. Left: Densities of states: total (dashed line); Lu (solid line); BC (dotted line). Right: BC FMO contributions for LuNiBC.

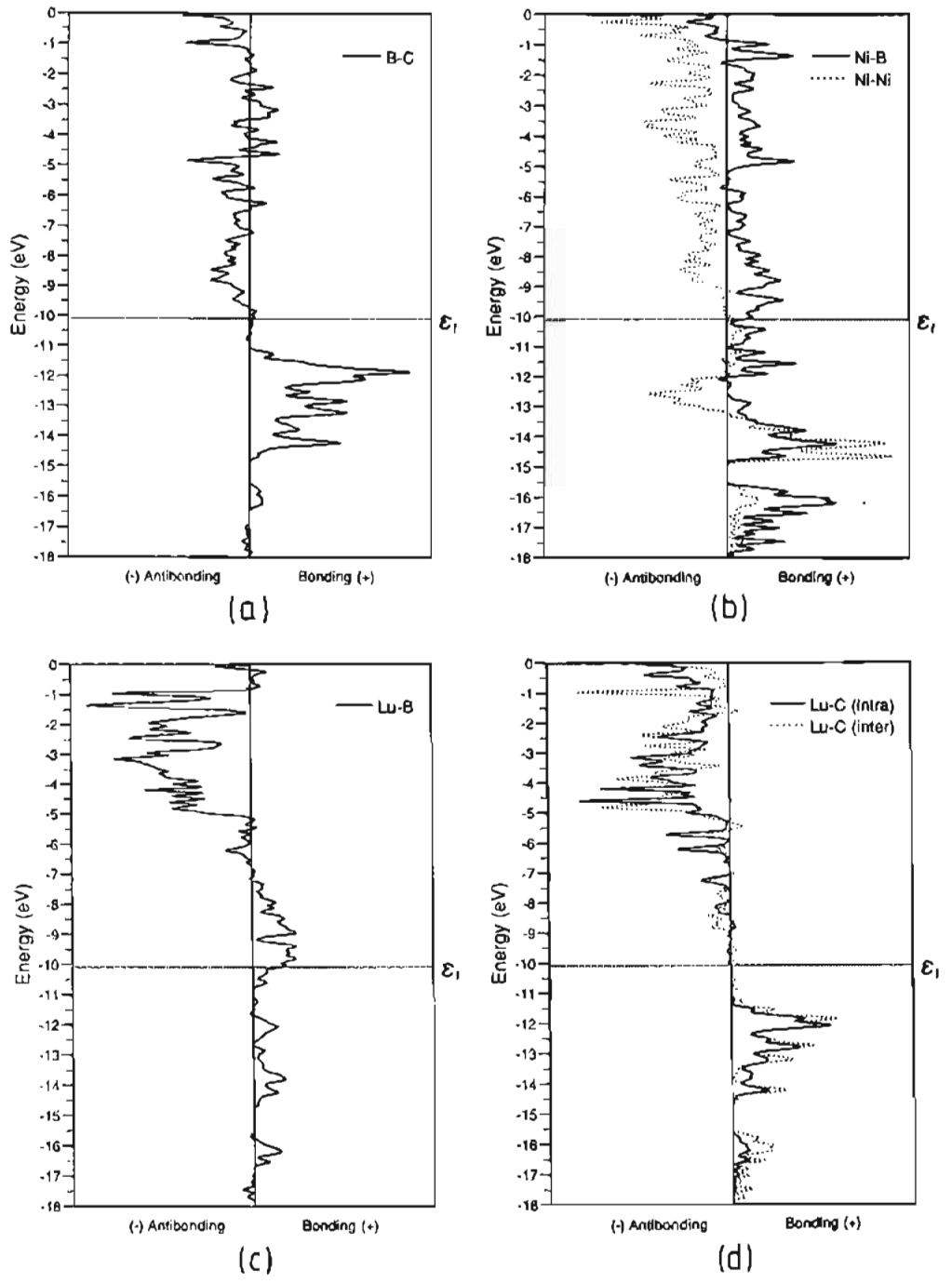

Figure 8. COOP curves for (a) B–C, (b) Ni–B (solid line) and Ni–Ni (dotted line), (c) Lu–B, and (d) intra Lu–C (solid line) and inter Lu–C (dotted line) contacts in LuNiBC.

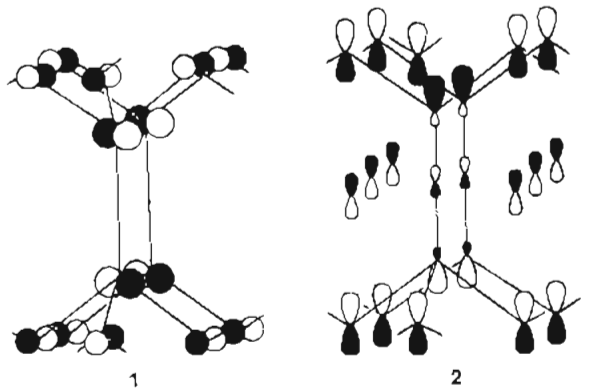

isostructural with $UCoC_2$[18] (see Figure 6). The atomic separations are comparable to those measured in $LuNi_2B_2C$, particularly the B–C distances (1.52 Å in LuNiBC vs 1.47 Å in $LuNi_2B_2C$). Note that the extra LuC sheet in LuNiBC leads to rather short Lu–C intersheet distances (2.437 Å), not present in $LuNi_2B_2C$. No report of this structural type with other lanthanides is known so far.

The MO diagram for an isolated BC unit is illustrated on the right-hand side of Figure 2. The AOs of B and C give rise to four σ-type combinations (one bonding, one antibonding, not shown in Figure 2, and two nonbonding noted 1σ and 2σ in Figure 2) and two degenerate bonding (1π) and antibonding (2π) combinations. The filling of the bonding and nonbonding MOs leads

(16) Simon, A. *Angew. Chem., Int. Ed. Engl.* **1991**, *30*, 1188.

(17) For an introduction to the COOP curves see: (a) Hughbanks, T.; Hoffmann, R. *J. Am. Chem. Soc.* **1983**, *105*, 3528. (b) Wijeyesekara, S. D.; Hoffmann, R. *Organometallics* **1984**, *3*, 949. (c) Kertesz, M.; Hoffmann, R. *J. Am. Chem. Soc.* **1984**, *106*, 3483.

(18) (a) Gerss, M. H.; Jeitschko, W. *Mater. Res. Bull.* **1986**, *21*, 209. (b) Li, J.; Hoffmann, R. *Chem. Mater.* **1989**, *1*, 83.

to a 10-electron species $(BC)^{3-}$ with a formal B–C triple bond, which makes it isoelectronic with $(C_2)^{2-}$, a unit often encountered buried in octahedral holes in solid state metal carbide compounds.[19] A HOMO–LUMO gap of 3.30 eV is computed for $(BC)^{3-}$. Such an anionic charge on BC leads to the formal oxidation state formalism $(Lu^{3+})(Ni^0)(BC)^{3-}$, somewhat comparable to the one for $LuNi_2B_2C$.

The DOS of LuNiBC is shown in Figure 7, for comparison with that of $LuNi_2B_2C$ given in Figure 3. Not so many differences are noticed. As for $LuNi_2B_2C$, a contribution from all the elements is present at $\mathcal{E}_F$. The position of $\mathcal{E}_F$ at −10.08 eV at the bottom of a rather broad band indicates that LuNiBC should also be metallic. The B and C contributions at the Fermi level are primarily due the participation of the nonbonding 2σ and to a lesser extent to the antibonding 2π FMOs. The rather important occupation of this 2π FMO and the depopulation of the bonding FMOs, particularly the 1π one (see Table 1), weaken the B–C bond strength after interaction. The B–C ovelap population, which was 1.441 in $(BC)^{3-}$ before interaction with the metallic host, drops to 0.977 after interaction. The B–C COOP curve represented in Figure 8 indicates that some B–C bonding states deriving from the BC 1π FMO are high in energy and vacant after interaction with the metallic framework. Note that rather strong interactions via Lu–C contacts are observed between the Lu–C sheets. The corresponding Lu–C overlap population is 0.394, larger than the intralayer one of 0.241. According to their corresponding COOP curves, they are maximized at the Fermi level (see Figure 8). Both are more important than the intralayer one measured for $LuNi_2B_2C$ (vide supra). The other atomic overlap populations are similar to those calculated for $LuNi_2B_2C$ (see Table 1 and compare Figures 4 and 8). This is the case also for the atomic net charges (see Table 1).

The band structure given on the right-hand side of Figure 5 indicates that the bands cut by the Fermi level are more dispersive than those for $LuNi_2B_2C$, particularly in the plane perpendicular to the stacking c axis. Conversely to the case of $LuNi_2B_2C$, flatter bands are present around the Fermi level along the line Λ ($\Gamma \rightarrow Z$), which corresponds to the [001] direction in the crystal.

Superconductivity Properties

If the $LnNi_2B_2C$ compounds are conventional superconducting materials,[8] their T_c is related to the density of states at the Fermi level.[20] Consequently, flat metal–non-metal bonding bands leading to a large DOS at the Fermi level might constitute one of the prerequisites for the obtention of the superconductivity phenomenon in the $LnNi_2B_2C$ materials. If it is so, superconductivity should be rather 2-D-like and should occur predominantly in the planes perpendicular to the stacking c axis, with a pairwise attraction occurring between the conduction electrons occupying these metal–non-metal bonding flat bands. The absence of superconductivity for LuNiBC might be associated with the rather weak DOS at the Fermi level, compared to that of $LuNi_2B_2C$. It is worthy of mention that no superconducting properties are observed for the related phase Lu_2NiBC_2, which also contains BC units.[21]

Concluding Remarks

Siegrist *et al.* reported that, with large and/or magnetic rare-earth metals, the superconducting state is not observed or decreases for the $LnNi_2B_2C$ phases.[4] These size and magnetic effects of the rare-earth-metal on the superconducting properties have already been noted for other materials such as the layered rare-earth-metal carbide halide compounds $Ln_2C_2X_2$.[16] Therefore, contrary to the case of the high-T_c oxocuprates,[22] the rare-earth-metal in the $LnNi_2B_2C$ phases seems to play a major role in the superconducting properties. In the nonsuperconducting $LaNi_2B_2C$ compound, for instance, an expansion and a contraction of the a and c axis are observed, respectively. The latter induces shorter B–C bond distances,[4,6] which might possibly perturb the shape and the nature of the DOS, particularly at the Fermi level, destroying the superconding state.

The EH calculations presented here show that the $LuNi_2B_2C$ and LuNiBC compounds are highly covalent and can be considered as intermetallic materials. Oxidation state formalisms of $(Lu^{2+})(Ni^0)_2(B_2C)^{2-}$ for $LuNi_2B_2C$ and $(Lu^{3+})(Ni^0)(BC)^{3-}$ constitute good starting points to describe their electronic structure. In $LuNi_2B_2C$, the Fermi level cuts a narrow and sharp peak in the DOS composed of mainly σ-type Ni–B bonding states. This allows us to conclude that electrons transferred from the $(B_2C)^{2-}$ entities into σ-type metal–non-metal bonding states are responsible for the superconducting properties of certain $LnNi_2B_2C$ phases. According to the band structure, flat bands are observed in the planes perpendicular to the stacking c axis. These materials should be 2-D-like superconductors somewhat comparable to the layered rare-earth-metal carbide halide compounds $Ln_2C_2X_2$.[16]

Acknowledgment. Thanks are expressed to Pr. J.-Y. Saillard for helpful comments and Pr. Rogl, Dr. L. F. Mattheiss, Dr. H. Noël, and Dr. M. Potel for providing results prior to publication.

(19) See for example: Long, J. R.; Halet, J.-F.; Hoffmann, R.; Meyer, H.-J.; Saillard, J.-Y. *New J. Chem.* **1992**, *16*, 839 and references therein.
(20) (a) Bardeen, J.; Cooper, L. N.; Schrieffer, J. R. *Phys. Rev.* **1957**, *108*, 1175. (b) Canadell, E.; Whangbo, M.-H. *Chem. Rev.* **1991**, *91*, 965.
(21) Zandbergen, H. W.; Cava, R. J.; Krajewski, J. J.; Peck, W. F., Jr. *J. Solid State Chem.* **1994**, *110*, 196.
(22) See for example: (a) Whangbo, M.-H.; Evain, M.; Beno, M. A.; Williams, J. M. *Inorg. Chem.* **1987**, *26*, 1832 and references therein. (b) Richert, B. A.; Allen, R. E. *Phys. Rev. B* **1988**, *37*, 7496 and references therein.